

Questions.

1. Should the theory be in this chapter, or in a separate theory chapter following the Lit. Review? If used in multiple chapters, or if mainly from literature, then it should be the latter.

Comments:

1. Section 4.1.1 needs to be better – it isn't clear what was done.  
– must discuss.
2. Try to minimize use of jargon acronyms (e.g. 'FBP') by careful phrasing and ordering of sentences.
3. Ensure thesis 'nomenclature' section describes all terms – it may need to be segmented by chapter if (x, y) etc. overlap a lot.

## Chapter 4

# Frame Localisation Optical

## Projection Tomography

Discuss.

In the previous chapters, volumetric imaging was achieved using widefield imaging and a relative scanning motion between the system's focal plane and the sample.

Volumetric imaging can also be achieved by rotating a sample and reconstructing tomographically. Accurate reconstructions of volumes rely on heavily on precision movement and rotation. Here an algorithm will be presented that relies exclusively on multiple (5+) tracked fiducial beads and reconstructs even with systematic mechanical drift. The algorithm presented will use an extension of the projective mathematics discussed in Chapter

(5+) or (5 or more)

OK: THIS SENTENCE NEEDS TO EXPLAIN  
HOW THIS CHAPTER IS A NATURAL PART  
OF THE THEORY.

4 tomographically  
5 reconstructing  
6 the 3D  
7 distribution  
8 of [fluorescence  
9 or brightness]  
10 signal  
11 within the  
specimen,

### 4.1 Tomography

Sharpe *et al* proposed Optical Projection Tomography in 2002 [?] using visible light to image transparent or translucent mesoscopic samples, with micro resolution. OPT addresses the scale gap between the PHOTOGRAPHIC techniques (samples larger than 10 mm), and light microscopy techniques (samples smaller than 1 mm) to image biological samples in the 1-10 mm regime. OPT is based on computerised tomography techniques [17] where set of projections of a sample are imaged as it travels through a full rotation. Algorithms exist to then transform this set of images into an xyz image stack. OPT is non-invasive optically but may require specialist invasive preparation for its samples. There are two imaging modalities for OPT, emission OPT (eOPT) and transmission OPT (tOPT). In eOPT, a fluorescent sample is

(OPT) give abbreviation

13  
14  
15 EFFECTIVE  
FOR  
16  
17  
18  
19  
20  
21  
22

a three-dimensional  
image stack  
in Cartesian (xyz)  
coordinates.

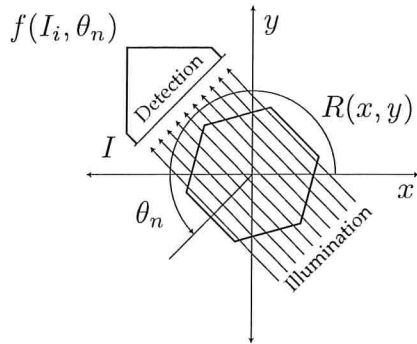


Fig. 4.1 Principle of OPT, a respective rotation between the sample and the detector illumination pair is iterated, the volumetric image is later reconstructed.

↳ from the set of captured 2D images,

- 1 excited using an illumination source off axis to the detection, similar to light-sheet but ✓
- 2 without the excitation being shaped into a sheet. Scattered illumination ✓
- 3 photons are rejected at the detector using an appropriate filter. In tOPT, a white-light ✓
- 4 source with a diffuser and a collimation is placed along the optical axis to provide ✓
- 5 near-collimated, uniform illumination onto the sample for transmission to a detector ✓
- 6 oppositely. See Figure 4.1. Each pixel at the detector corresponds to a ray that has passed. ✓
- 7 through the sample whose intensity has been attenuated by the sample. The two modalities can work in unison to provide contextual information, the transmission ✓
- 8 images provide overall structure which can be supplemented by the fluorescent ✓
- 9 signal from a label of interest. ✓
- 10 indicating (OPTICAL DENSITY OF ABSORPTION OR SCATTERING) with ✓

### 4.1.1 Reconstruction

- 11 As the sample is rotated each pixel collects an intensity  $I = I_0 e^{-k}$  at discrete angles  $n$  through a full rotation of the sample; where  $I_0$  is the unattenuated radiation intensity from the source to the detector,  $k$  is the attenuation caused by the sample along a detected ray and  $I(\theta)$  is the measured intensity, see Figure Rays from the sample to the detector approximate straight lines, and so the rays reaching the detector with a line integrals. A projection is then the resulting intensity profile at the detector for a rotation angle, and the integral transform that results in  $f(I_i, \theta_n)$  is the Radon transform. This is defined mathematically as:

Let's discuss.  
- Surely it is not  $I_0$ , since  $\theta$  is sample rotation.

- The  $k$  might be  $k_\theta$ , however.

$$f(I_i, \theta_n) = \int \int R(x, y) \delta(x \cos(\theta_n) + y \sin(\theta_n) - I) dx dy \quad (4.1)$$

$\cos, \sin$  are non-italic, as operators.

What is  $R$ ?

WHY  $I$ ?

Never use it's, which means it is

## 4.2 Stereoscopic Imaging

49

Where  $f(I, \theta)$  is the Radon transform, and  $R(x, y)$  represents a 2D slice of the sample. A parallel projection is then just the combination of line integrals  $f(I)$  for a constant  $\theta$ . An inverse Radon transform is used to recover the original object from the projection data. By taking the Fourier transform of each projection measurement and reorder the information from the sample into its respective place in Fourier space. This is valid due to the Fourier Slice theorem () which states that the Fourier transform of a parallel projection equivalent to a 2D slice of the Fourier transform of the original sample. A spatial filtering step is applied during back-projection to avoid spatial frequency oversampling during the object's rotation (see Figure) a high pass filter is commonly used to compensate for the perceived blurring. FBP can be thought of as smearing the projection data across the image plane, and is expressed in equation form as:

- 1 represents what? optical density?
- 2 'signal'?
- 3 IF NOT
- 4 THEN f
- 5 MAY NOT
- 6 DIRECTLY
- 7 BE A
- 8 BRIGHTNESS.
- 9
- 10
- 11
- 12
- 13
- 14
- 15
- 16
- 17
- 18
- 19
- 20
- 21
- 22
- 23
- 24
- 25
- 26
- 27
- 28
- 29

$$R_{fpp}(x, y) = \int_0^\pi f'(x \cos(\theta) + y \sin(\theta), \theta) dx dy \quad (4.2)$$

where  $f'$  is the filtered projection data, and  $R_{fpp}$  is the back-projected image.

(4.3)

15

16

17

### Aim

The Radon transform relies heavily on the assumption of circular motion only. This chapter hopes to exploit some of the techniques seen in stereoscopic imaging to register back projections rather than relying on line integrals. The algorithm proposed here is therefore robust to mechanical drifts across acquisitions as well as inconsistent angular steps

with constant angular steps about a vertical axis.

19

20

21

22

23

24

## 4.2 Stereoscopic Imaging

features

25

26

27

28

29

Imaging scenes in stereo allows for the triangulation of individual points in 3D space, features or fiducials in one detector to another. Triangulation requires features in both images to be the same; this is known as the correspondence problem. Many methods exist to ensure that features are known and confidently the same between

detected and accurately associated

to be uniquely

detected in both images

of a stereo imaging system,

and for these detections

to be correctly associated with one another.

when the  
features are  
uniquely identifiable  
points such as  
fluorescent beads.

50

## Frame Localisation Optical Projection Tomography

- image data from two cameras.* New sentence. Say more, if possible to do so concisely based on a review paper.
- 1 two cameras; properties of scale independent features and their surrounding pixel environment in one image can be matched to a similar feature in the second image.
  - 2 Now, suppose we know the relative positions of the two cameras and their
  - 3 intrinsic parameters. Given the CCD parameters, we can translate pixel coordinates

5  $(u, v)$  into image plane coordinates  $(x, y)$ :

$\uparrow \uparrow$   
use italic.

$$u = u_0 + k_u x$$

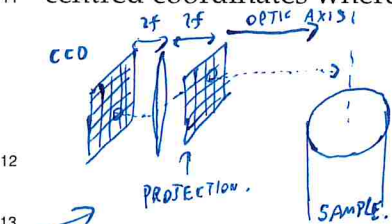
$$v = v_0 + k_v y$$

DON'T MIX UP  $(x, y)$  For image plane with  $(x, y)$  for specimen reconstruction  
(4.4) in fig. 4.1

(4.5)  $(x, y)$  is in

the specimen frame of reference.

- 9 And knowing the focal length of the imaging system, image plane coordinates  
10 may be translated into a ray in 3D. The ray can be defined by a point  $p$  in camera-  
11 centred coordinates where it crosses the image plane as:



WHERE IS THE IMAGE PLANE?  
- SURELY THE SAMPLE  
IS IMAGED PROJEKTIVELY...

SHOULD DISCUSS.

$$\mathbf{p} = \begin{bmatrix} x \\ y \\ z \end{bmatrix}$$

I THINK THIS WILL NEED A DIAGRAM, WITH CO-ORDINATE SYSTEMS, TO EXPLAIN.  
(4.6)

- 13 From the definition of a point as observed through an image we can construct  
14 a dual-view model of points in space. Using a model of a system with two views  
15 allows for the triangulation of rays based on image correspondences, this is an  
16 important part of stereovision. The most important matching constraint which can  
17 be used is the *epipolar constraint*, and follows directly from the fact that the rays must  
18 intersect in 3D space. Epipolar constraints facilitate the search for correspondences,  
19 they constrain the search to a 1D line in each image. To derive general epipolar  
20 constraints, one should consider the epipolar geometry of two cameras as seen in  
21 Figure ??

22 The **baseline** is defined as the line joining the optical centres. An **epipole** is the  
23 point of intersection of the baseline with the image <sup>plane</sup> and there are two epipoles,  
24 one for each <sup>camera</sup>. An **epipolar line** is a line of intersection of the epipolar plane  
25 with an image plane. It is the image in one camera of the ray from the other camera's  
26 optical centre to the point X. For different world points X, the epipolar plane rotates  
27 about the baseline. All epipolar lines intersect at the epipole. <sup>definition (?)</sup>

28 The epipolar line constrains the search for correspondence from a region to a line.  
29 If a point feature  $x$  is observed in one image, then its location  $x'$  in the other image  
30 must lie on the epipolar line. We can derive an expression for the epipolar line. The

I THINK THIS SENTENCE IS CLEAR, BUT I THINK AT THERE ARE 'IMAGES' AND 'IMAGE PLANES' IN THIS CHAPTER. SO 'FRAME OF IMAGE DATA' MAY BE NEEDED.

## 4.2 Stereoscopic Imaging

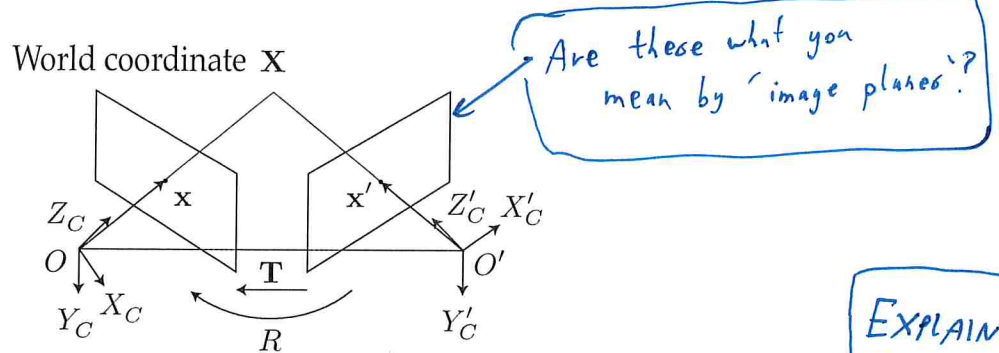


Fig. 4.2 Epi-polar geometry described for two adjacent views (or cameras of a scene).

??

two camera-centered coordinate systems are related by a rotation  $R$  and translation

T:

Do you mean  $x = Rx' + T$  or  $x' = Rx + T$

( $\because X_c'$  is an axis!  $X'$  is a position.)

$$X'_c = RX'_c + T$$

ARE BOTH PRIME (?!)

Taking the vector product with T, we obtain

IF THIS IS WRONG, IT IS  
AWFULLY WRONG, BUT POSSIBLY  
IT DESCRIBES THE EPIPOLE (ONLY)  
 $T \times X'_c = T \times RX'_c + T \times T$

$$T \times X'_c = T \times RX'_c$$

IN WHICH CASE,  
NEEDS A NICELY  
WORDED INTRO SENTENCE.

GIVE  
(EQUATION #)

FOR ALL EQUATIONS.

- READER MAY WISH TO  
REFER TO ONE YOU  
DON'T NUMBER.

$$(4.7a) \quad (4.7b)$$

$$(4.7)(4.7)$$

3

4

5

6

7

9

10

11

12

13

14

15

16

? (4.2.1) Essential Matrix for (?)

Taking the scalar product with  $X'_c$ , we obtain:

$$X'_c \cdot (T \times X'_c) = X'_c \cdot (T \times RX'_c)$$

$$X'_c \cdot (T \times RX'_c) = 0$$

A vector product can be expressed as a matrix multiplication:

$$T \times X_c = T \times X_c \quad (4.8)$$

↑

WHY SUBSCRIPT 'X' HERE?

1 where

$$2 \quad T_x = \begin{bmatrix} 0 & -T_z & T_y \\ T_z & 0 & -T_x \\ -T_y & T_x & 0 \end{bmatrix} \quad (4.9)$$

3 *WHY  $r_x$ ? NOT JUST  $T$ ?*

4 So equation (??) can be rewritten as:

5  $\mathbf{X}'_c \cdot (T_x R \mathbf{X}_c) = 0$

6  $\mathbf{X}'_c T E \mathbf{X}_c = 0$

7 *DOE IS THIS INTENDED TO SUPPORT (3D) ROTATION, OR JUST WITH A ABOUT AN ALIGNED Z-AXIS? I ASSUME THE FORMER... HENCE THE PROGRESSION?*

where

8

$$9 \quad E = T_x R$$

11 E is a  $3 \times 3$  matrix known as the *essential matrix*. The constraint also holds for  
12 rays  $\mathbf{p}$ , which are parallel to the camera-centered position vectors  $\mathbf{X}_c$ :

13

$$14 \quad \mathbf{p}'^T E \mathbf{p} = 0 \quad (4.10)$$

15 This is the epipolar constraint. If we observe a point  $\mathbf{p}$  in one image, then its position  
16  $\mathbf{p}'$  in the other image must lie on the line defined by (4.10). The essential matrix can  
17 convert from pixels on the detector to rays  $\mathbf{p}$ , assuming a calibrated camera. And  
18 pixel coordinates can then be converted to image plane coordinates using:

19

$$20 \quad \begin{bmatrix} u \\ v \\ 1 \end{bmatrix} = \begin{bmatrix} k_u & 0 & u_0 \\ 0 & k_v & v_0 \\ 0 & 0 & 1 \end{bmatrix} \begin{bmatrix} x \\ y \\ 1 \end{bmatrix} \quad (4.11)$$

*DISCUSS - IN THE SPECIMEN?*

*BUT ARE WE 'IMAGING' PROJECTIVELY?*

## 4.2 Stereoscopic Imaging

We can modify this to derive a relationship between pixel coordinates and rays:

$$\begin{bmatrix} u \\ v \\ 1 \end{bmatrix} = \begin{bmatrix} \frac{k_u}{f} & 0 & \frac{u_0}{f} \\ 0 & \frac{k_v}{f} & \frac{v_0}{f} \\ 0 & 0 & \frac{1}{f} \end{bmatrix} \begin{bmatrix} x \\ y \\ f \end{bmatrix} \quad (4.12)$$

If we define the matrix  $K$  as follows:

$$\underbrace{\boldsymbol{K}}_{\text{bold}} = \begin{bmatrix} fk_u & 0 & u_0 \\ 0 & fk_v & v_0 \\ 0 & 0 & 1 \end{bmatrix} \quad (4.13)$$

then we can write

*WHAT BOLD / ITALIC CONVENTION ARE YOU USING?*

$\rightarrow$  I think  $K$  should be bold (italic optional)

$\rightarrow$  Its elements ( $fk_u$ ) need not be  $\rightarrow$  they can be italic, only.

$$\tilde{\mathbf{w}} = K\mathbf{p} \quad (4.14)$$

(4.2.2) Fundamental Matrix for  (?)

$\leftarrow$  where  $\tilde{\mathbf{w}}$  is ....

The epipolar constraint becomes

$$(4.15) \quad \mathbf{p}'^T E \mathbf{p} = 0$$

$$(4.16) \quad \mathbf{p}'^T E K^{-1} \tilde{\mathbf{w}} = 0$$

$$(4.17) \quad \tilde{\mathbf{w}}'^T K^{-T} E K^{-1} \tilde{\mathbf{w}} = 0$$

$$(4.18) \quad \tilde{\mathbf{w}}'^T F \tilde{\mathbf{w}} = 0$$

The  $3 \times 3$  matrix  $F$

$F$  is called

$F$  is the  $3 \times 3$  fundamental matrix.

With intrinsically calibrated cameras, structure can be recovered by triangulation.

Firstly the two projection matrices are obtained via a singular value decomposition of the essential matrix. The SVD of the essential matrix is given by:

$$\hat{T}_x = U \begin{bmatrix} 0 & 1 & 0 \\ -1 & 0 & 0 \\ 0 & 0 & 0 \end{bmatrix} U^T \text{ and } R = U \begin{bmatrix} 0 & -1 & 0 \\ 1 & 0 & 0 \\ 0 & 0 & 1 \end{bmatrix} V^T \quad (4.19)$$

Then, aligning the left camera and world coordinate systems:

$$P = K[I|0] \text{ and } P' = [R|T] \quad (4.20)$$

*WHY AREN'T THESE DEFINED (?!?) IF THEY ARE THE PROJECTION MATRIXES THEN THIS NOT-EXPLICIT PHASE IS NOT ADEQUATE TO SAY SO.*

- Given the two projection matrices, we can recover structure (only up to scale, since  $|T|$  is unknown) using least squares. Ambiguities in  $T$  and  $R$  are resolved by ensuring that visible points lie in front of the two cameras. As with the essential matrix, the fundamental matrix can be factorised into a skew-symmetric matrix corresponding to translation and a  $3 \times 3$  non-singular matrix corresponding to rotation.

→ So Far, this could be theory following Literature Review. //

### 4.3 The proposed algorithm

- During a typical OPT acquisition, a fiducial will appear to follow an elliptical path in  $(x, y)$ . In the following volume reconstruction there will then be a fitting step to recover the path of the fiducial, to then apply a correction before applying a radon transform. This type of reconstruction not only ignores any mechanical jitter of the sample but also any systematic drift.

We have seen that using two adjacent images of a scene separated by some rotation and translation, points in 3D space may be triangulated within the scene given the rotational and translational matrices of the respect camera views. The inverse is also possible, given a sufficient amount of known fiducial points in a scene the translation and rotation matrices can be recovered. The recovery over a more exact description of the motion of the scene can eliminate any need for a fitting and may recover and correct for drift as well as eliminate any mechanical jitter. Errors may however then be introduced from fiducials mechanically slipping and localisation errors. The shift of a camera or a camera pair around a scene separated by a translation matrix is analogous to a sample moving in the fixed view of an imaging detector, like in OPT.

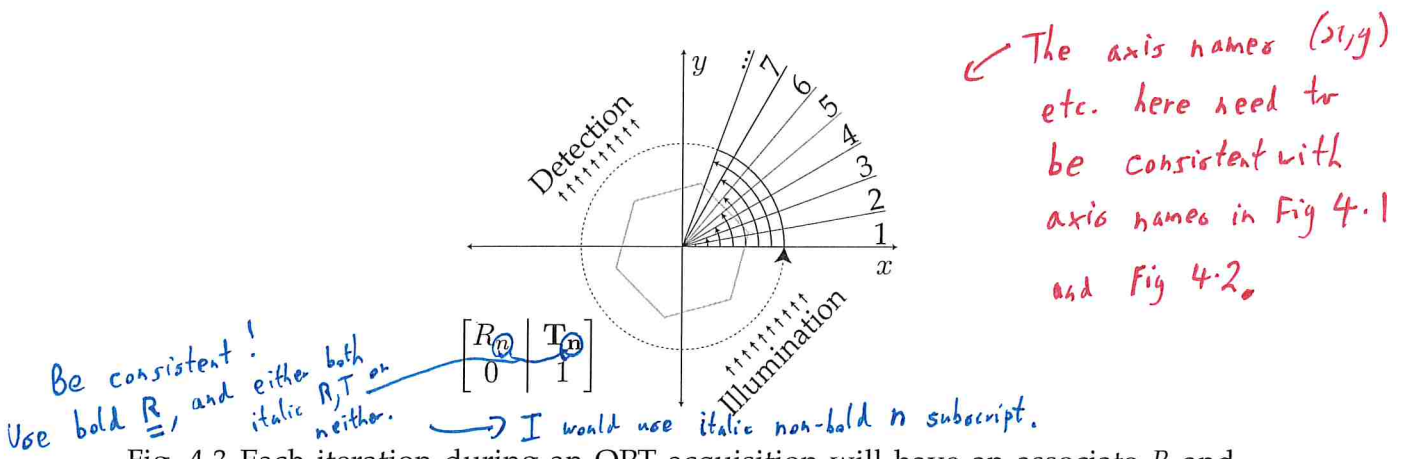
Once a sufficient amount of fiducials are reliably tracked from the first to the second image, the Fundamental, Essential or Homography can be computed. Using the factorisation one of these matrixes between each adjacent view of a rotating scene the translation and rotational matrices may be recovered. Here we will discuss a reconstruction using  $F$  but the same principle applies for  $E$  and  $H$ .

and (?)      matrixes

PROBLEM:  
YOU NEED  
TO DISTINGUISH  
  
(x, y)-CAMERA 1  
(x', y')-CAMERA 2  
(x, y)-SPECIMEN  
FRAME.  
  
BUT NOW,  
WE DON'T  
SEEM TO  
HAVE 2  
CAMERAS....

about what it  
accounts for...  
↓  
IT WON'T  
ACCOUNT FOR  
EVERYTHING  
(e.g. PARTIAL  
SAMPLE  
MELTING),

I THINK THIS MAY NEED TO BE AT THE START  
OF THIS SECTION, TO RELATE 2-CAMERA TO  
OPT... ]



The axis names ( $x, y$ ) etc. here need to be consistent with axis names in Fig 4.1 and Fig 4.2.

Fig. 4.3 Each iteration during an OPT acquisition will have an associate  $R$  and  $T$ , these matrices can be recovered from comparing the current iteration to the previous iteration.

Here are two ways of reconstructing using the Fundamental matrix as described above. The first method involves computing  $F$  for two neighbouring images with 5 or more fiducials, having more beads helps to remove ambiguity and increase confidence in  $F$ . Once  $F$  is calculated  $F$  is then decomposed into  $R_n$  and  $T_n$  between each view  $n$  and  $n + 1$ . The image at view  $n + 1$  is then back projected along the virtual optical axis within a virtual volume where the sample will be reconstructed. The size of this back projection and virtual volume is chosen to be suitably large (so that important data is not lost). Then, all the prior rotation and translation matrices are serially multiplied from  $[R_0 | T_0]$  until  $[R_n | T_n]$ , this final matrix is inverted and applied to the back projected volume. The matrix inversion step is important as it realigns the back projection in the volume to where it originally was compared respective of the first projection. This process is repeated for every angle and the back projected volume from each step is summed with every other step. Finally the remaining volume is filtered using a high-pass filter; here a Ram-Lak filter is used.<sup>1</sup> By producing a series of transformation matrices from adjacent acquisitions, errors compound and the reconstruction of volumes degrades with more projections, see Figure ??.

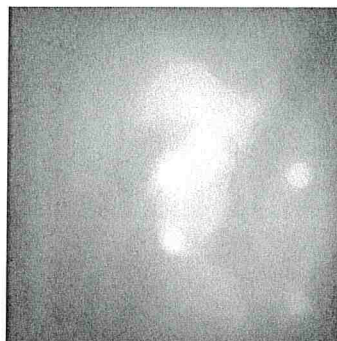
The following approach is less prone to compound errors but relies on precise fiducial distinction and tracking. Instead of calculating  $F$  between neighbouring images  $F$  is calculated between the current projection and the very first projection.  $F$  is then decomposed and the transformation matrix is inverted and applied to the back projected volume. The reoriented back projected volumes are summed and

<sup>1</sup>Linear ramp filter in Fourier space:  $|v|$

Phase ramp or amplitude ramp?

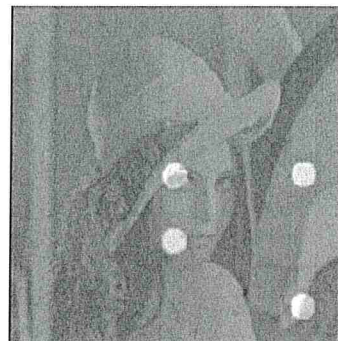
what is  
[R | T] ?  
what does it  
mean?

identification  
and  
tracking  
of  
fiducial  
markers



i.e. a reconstruction.

(a) Unfiltered output of the radon transform



(b) Ram-lak (Fourier ramp) filter applied to Figure 4.4a.

Fig. 4.4 The result of an Tomographic reconstruction requires Fourier filtering to normalise spatial contrast

This shows a reconstruction, using  
 (a) a basic and (b) a new method.  
 You need to show how the input data for these analyses were obtained.

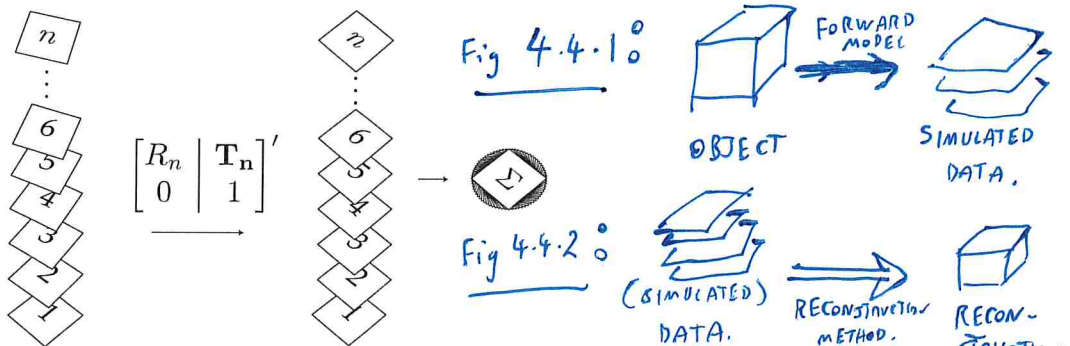


Fig. 4.5 Two dimensional representation of the reconstruction algorithm. The rotational and translation matrices are recovered and inversely applied to back projected images. The now realigned back projection are summated to produce an unfiltered back projection.

- 1 finally filtered to remove the additional spatial frequencies imparted from rotating the sample.
- 2 The second approach may be is more robust to compound errors but an additional programmatic step is needed to know which beads in the first image correspond to beads in the current image. This can be achieved using standard tracking and momentum particle tracking algorithms. In both cases a decomposed  $F$  will produce four possible transformation pairs. Once the transformation matrix between the first view and the second view is calculated the proceeding transformation matrices are then easily chosen by similarity and general direction of motion. An example of this

in the n<sup>th</sup> image.

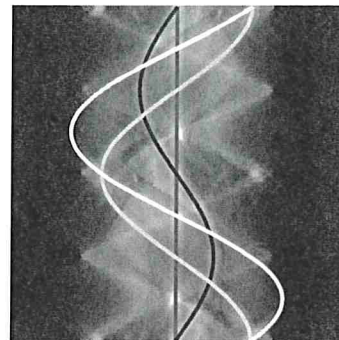
(but the task is more challenging than tracking between consecutive frames due to the

increased problems of intermittent signal dropout – e.g. if a particle moves too far away from the system's focal plane).

**bold + Non-bold fails to show up in the main text.**



(a) Raw input for OPT simulations, Lena.



(b) Image of Lena (Figure 4.6a) after rotation and projection in 2D, giving the sinogram. ↗

IS THIS THE  
GIVE DIAGRAM  
SHOWING HOW THE  
SIMULATED OBJECT  
WAS ROTATED TO  
PRODUCE THIS.  
LABEL AXES.

Fig. 4.6 Reference images for OPT reconstruction.

Aarg! This should  
be explained before  
the reconstruction.

Also, I  
assume it  
is in  
3D...  
Eg.

type of selection would be:

$$\min_{I(n)} I(n) = ([R_n | T_n] - [R_{n-1} | T_{n-1}])^2 \quad (4.21)$$

The first two views are more difficult to choose the correct decomposition form but it is possible if a suitable ideal matrix is given as a comparison. Such an ideal matrix is composed using *a priori* knowledge of the likely angle of rotation of the system's imaging properties.

## 4.4 Results

To verify the proposed algorithm successfully reconstructs as theorised, it was applied to simulated data. The image of Lena<sup>2</sup> is used here as a test image to verify the validity of each reconstruction. Superimposed on Lena are fiducial beads to track the rotation of the image, see Figure 4.6a. The reference image was then rotated through 128 angles over  $2\pi$  radians and projected along the  $y$  axis and a slice in  $xy$  was taken to create a single line projection. This is repeated for each angle with each line projection stacked to create a sinogram, see Figure 4.6b.

<sup>2</sup>The image of Lena is used as a reference to a very early full colour digital scanner. The researchers in question realised that their presentation of the scanner's capabilities at a conference lacked a test image. The nearest image to hand was a Playboy magazine with Lena Söderberg as the centrefold.

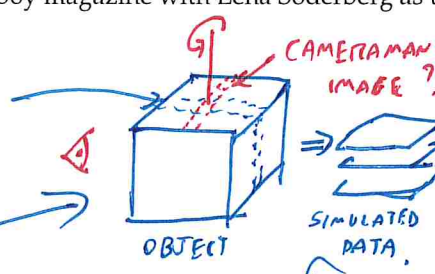
i.e. the  
process of  
producing  
simulated image  
data.  
This is  
"Methods"  
not results.  
Cah  
discuss.

PROBABLY  
NOT NEEDED.  
JUST  
"STANDARD  
REFERENCE  
IMAGE DATA".  
→ DELETE.

IS THIS THE  
SIMULATION  
METHOD?

Since this chapter is on  
theory, I think it is essential to  
know if the proposed method works  
for this type of data as well as the effectively 2D  
data.

Lena  
Image.



WHAT ABOUT  
IF YOU ADD A  
SECOND FEATURE,  
AT 90°, TO PREVENT  
THE EXAMPLE BEING  
OVER-SIMPLIFIED.

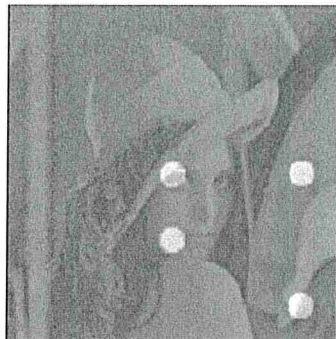


Fig. 4.7 Reconstruction of a reference image using the new proposed algorithm

FLOWCHART DIAGRAM (?).

In the standard ~~algorithmic~~ approach for OPT, the sinogram produced then undergoes the Radon transform, see Figure 4.4a and then a post filtering, see Figure 4.4a. This step is substituted for the proposed algorithm; in Figure 4.8 the two techniques are compared for ideal conditions of smooth, predictable rotation. The proposed algorithm produces (see Figure 4.7) a faithful reconstruction on the original image, with some minor deviations. Both techniques lose some of the original contrast of the image due to under-sampling of rotations. When taking the histogram of the absolute pixel-wise difference between the original source image to the images produced by the new algorithm and the Radon transform, there is a clear shift to less discrepant pixels for the new algorithm. This would suggest that the new algorithm is producing a more accurate interpretation than the standard radon transform, see Figure 4.9.

The more challenging case of a sample drifting systematically along the x axis was then considered, this produced a helical path of a single fiducial within the sample, see Figure 4.10a. In Figure 4.11a, the Radon transform entirely fails to produce a recognisable reproduction of the test image with the addition of a slight helicity to the rotation. The proposed algorithm produces an equivalent result to that of a sample rotating without any systematic drift, see Figure 4.4b. In Figure 4.12 the respective images from each algorithm were compared as before while the helical shift was incremented. See Figure 4.10a for a sinogram of a sample whereby a helical shift has been induced. When using correlation as a metric of reproduction quality, at zero helicity, the new algorithm fairs slightly worse at 94% correlation compared to the Radon transform at 96%. As expected, the Radon transform rapidly deteriorates once a systematic drift is applied; whereas the new algorithm maintains quality of reconstruction, see Figure 4.12.

Try decrease of [say] 20% in the p.m.s. pixel value variance of the pixel values... error of the pixel values, (give equation used to express this error, e.g.)

$$\epsilon = \frac{\sum_i (I_i^{\text{recon}} - I_i^{\text{true}})^2}{\sum_i (I_i^{\text{true}})^2}$$

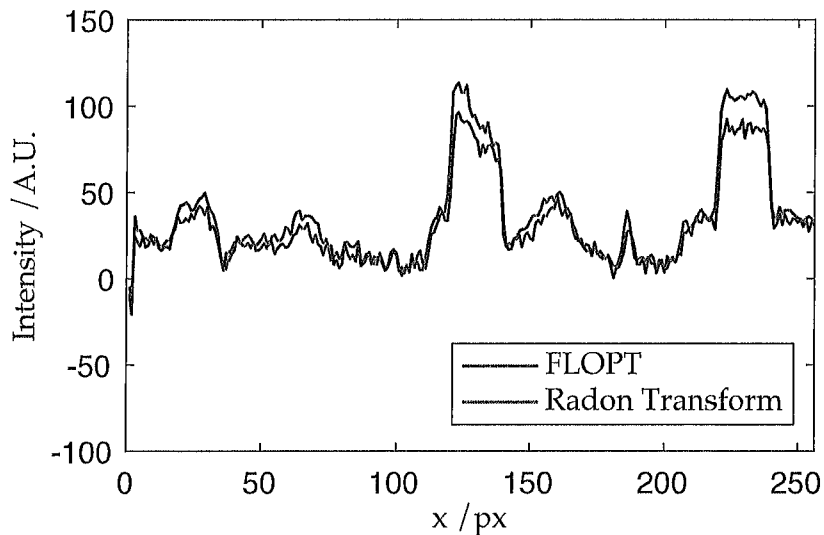


Fig. 4.8 Line profile comparison of the reconstruction of a reference image artificially rotated and projected using the standard radon transform and the new proposed algorithm.

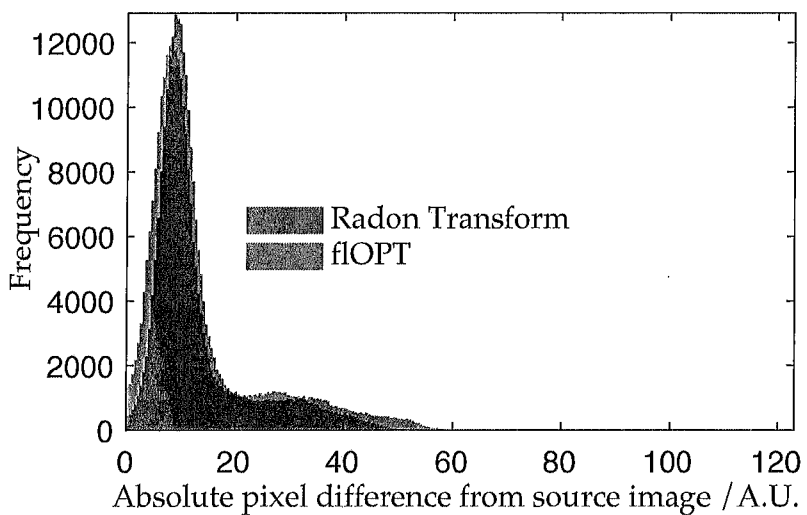


Fig. 4.9 Histogram of of pixel values compared between reconstructions using fLOPT and the Radon transform. The shift of the histogram to towards overall lower deviance from the source image suggests the fLOPT algorithm out performs the radon transform

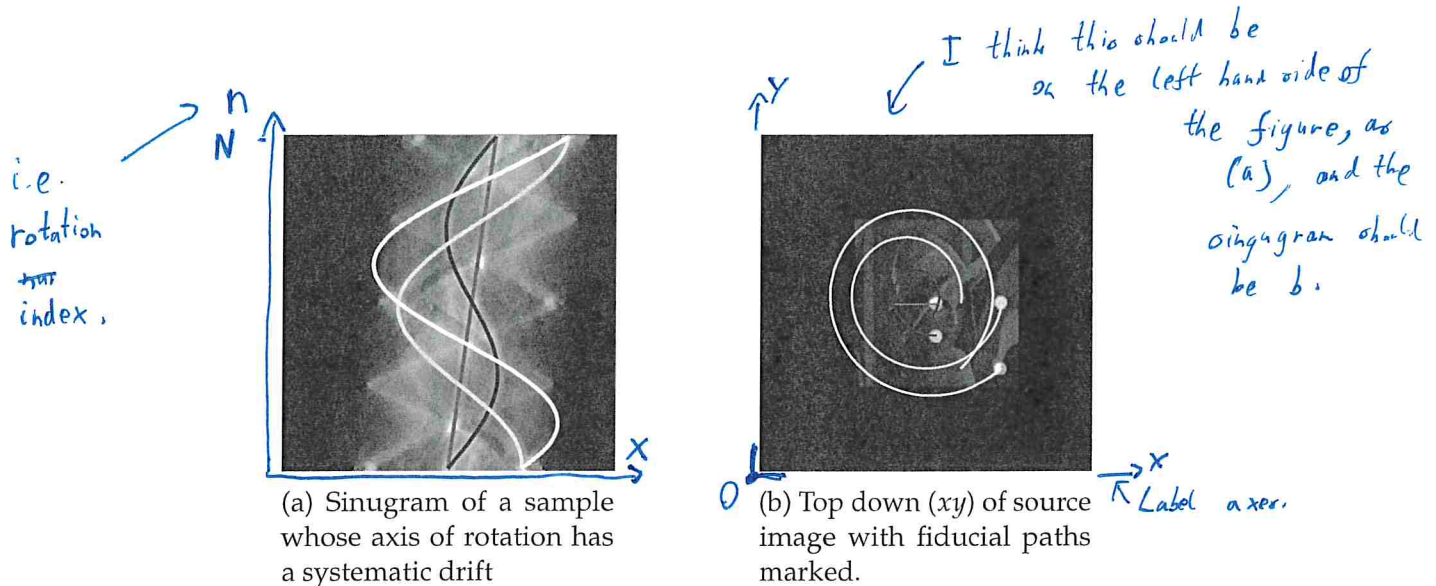


Fig. 4.10 Comparison of the two reconstructions under sample imaging with a systematic drift, in 3D though represented here in 2D.



Fig. 4.11 Comparison of the two reconstructions under sample imaging with a systematic drift, in 3D though represented here in 2D.

Ok, clearly a good improvement.  
Is this definitely new?  
→ Is there a risk of finding this method in literature?  
→ Seems like a risk, so please check carefully.

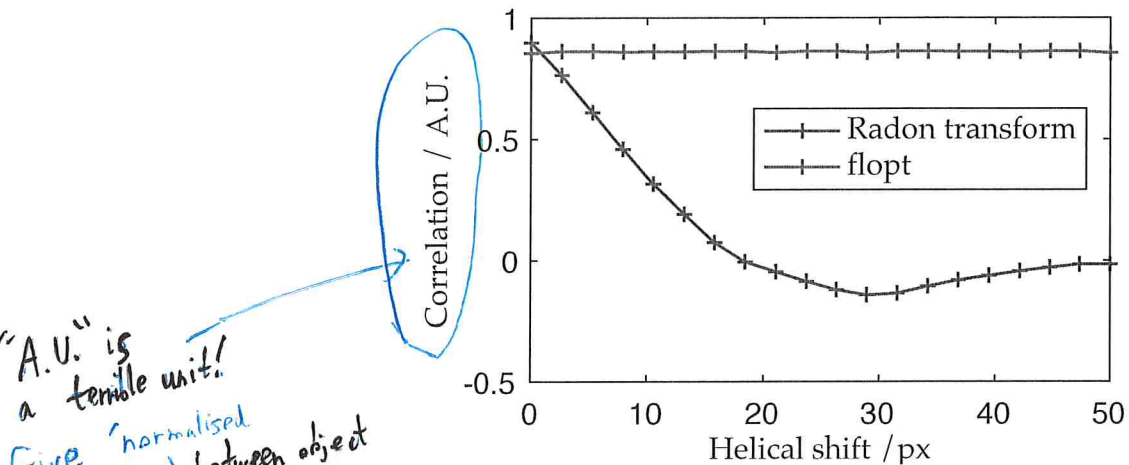


Fig. 4.12 2D correlation of the source image shows that fOPT does not degrade under systematic drift compared to Radon Transforms.

### Recovery of R and T using matrix decomposition *bold?*

To quantitatively verify that the matrix decomposition technique was valid and robust, the accuracy of the reproduction of  $R'$  and  $T$  was tested directly. The original  $R$  and  $T$  matrices were computed and compared to  $R$  and  $T$  generated from matrix decomposition, this absolute difference was computed element-wise in each matrix and then an average for each matrix was taken. Overall the worst case scenario produced a percentage error of 2% see Figure 4.13 for full statistics. The accuracy of the calculated  $R$  and  $T$  did deteriorate when adding in additional degrees of combined movement, but the severity of this movement appeared to no trending effect. Consistently the translational matrix was more accurately reproduced, this is likely due to there being fewer of degrees of freedom for errors to spread over.

What does this mean?

## 4.5 Discussion

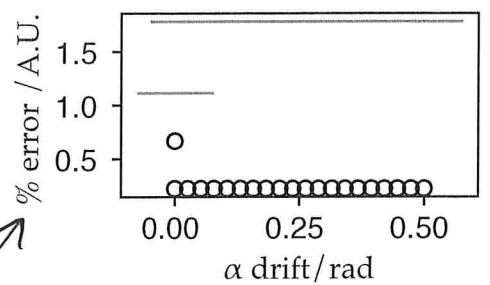
A new algorithm for reconstructing OPT data has been demonstrated. The new algorithm uses multiple fiducials to recover the matrix which describes the rotation and translation. The quality of the reconstructions when compared to a standard radon transform shows a slight improvement, with a great effect when a systematic drift is introduced. When comparing the expected matrices to the recovered matrices a peak of 2% difference is found between the two when considering worst case scenarios; suggesting the technique is robust to all forms of drift and general

*need to state, near start of chapter, that 'fiducials' means an accurately locatable fiducial marker, in this chapter.*

2% is quantitative.  
Hence need to define equation w.r.t to obtain it!

'ground truth' to the reconstruction'

The word alone doesn't have a precise enough technical meaning until you state one for the purposes of the chapter.



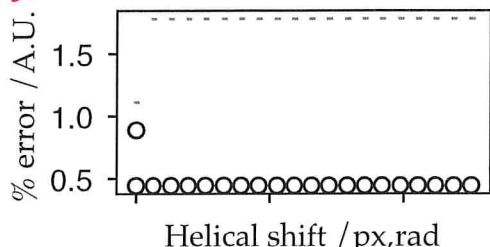
(a) Rotation matrix, with angular drift in  $\alpha$

five  
matrix  
% error in  
what?  
relative error  
in angle?

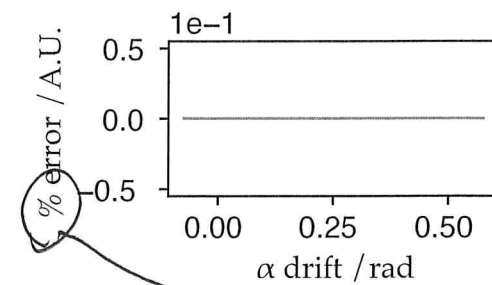
A percentage cannot

be in  
arbitrary units!  
It must have

(c) Rotation matrix, with helical drift in  $x$  only



(e) Rotation matrix, with angular drift in  $\alpha$  and helical drift in  $x$



(b) Translation matrix, with angular drift in  $\alpha$

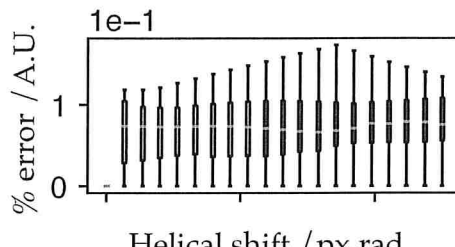
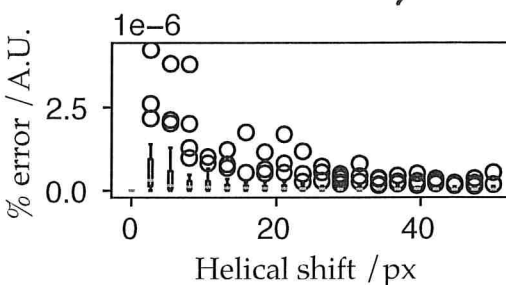


Fig. 4.13 Box plots demonstrating that the Rotational and Translations matrices can be recovered accurately from fiducial marker positions. Panels 4.13a and 4.13b introduce an angular drift during rotation, to an observer at the detector this would appear as a tip of the sample towards them, causing precession. Panels 4.13c and 4.13d introduce a lateral drift in  $x$  causing a helical path to be drawn out. Panels 4.13e and 4.13f combine the two effects. In all cases the percentage error introduced by the addition of undesirable additional movements was on the order of < 2%.

instability. Such an algorithm could be used to help in minimising ghosting effects seen in real samples; particularly in samples where slipping is likely to occur such as in gels or in cheaper OPT systems which tend to be more mechanically unstable and imprecise.

#### 4.5.1 Future work

##### Bead Tracking

The work presented here is, so far, is only proof-of-concept and requires several steps in order apply it to real OPT data. Firstly, a full bead-tracking algorithm will need to be created to track multiple beads concurrently in an image series. A sensible approach would be to have a user select the fiducials in the image on the first frame and template match in a small window around the selection; this is similar to the algorithm described in Chapter Template matching is robust to occlusions provided the fiducial is not fully eclipsed. If two fiducials occlude each other however, this algorithm may switch their identities or both tracking windows may follow one bead. This is a common problem in particle tracking algorithms but is essentially solved by using a weighted likelihood based on momentum.

The likelihood of a bead occlusion occurring will increase with the introduction of additional beads into the sample. As such occluded beads may need to be omitted and possibly interpolated for. Egregious outliers may be found by tracking a confidence estimator as the bead rotates. A primitive estimator would be the pixel-wise sum of intensities in the result of a correlative template matching. Whilst this confidence value itself has no physical interpretation, any stark changes in the derivative will be suggestive of an occlusion or mis-tracking of some variety, see Figure 4.14.

##### Multiple Views Tracking

The theory backing the proposed algorithm relies on triangulation between two view points. However, it is possible to use three separate views to reconstruct a scene, one such approach being used quaternion tensors. Working with tensors is computationally and mathematically more challenging, but a future iteration of the algorithm presented here may benefit from using three views to provide a more accurate transformation matrix. Beyond three views there currently is no

<sup>1</sup>  
<sup>2</sup>  
<sup>3</sup>  
<sup>4</sup>  
<sup>5</sup> demonstrated by simulation  
<sup>6</sup> and reconstruction from ground-truth testcard objects.  
<sup>7</sup>  
<sup>8</sup>  
<sup>9</sup>  
<sup>10</sup>  
<sup>11</sup>  
<sup>12</sup>  
<sup>13</sup>

<sup>14</sup> CAN  
<sup>15</sup> OFTEN BE  
<sup>16</sup> IT IN  
<sup>17</sup> LITERATURE  
<sup>18</sup> REVIEW)

<sup>24</sup> I don't see what this means I add  
<sup>25</sup> → delete.

<sup>26</sup>  
<sup>27</sup>  
<sup>28</sup>  
<sup>29</sup>  
<sup>30</sup>  
<sup>31</sup>  
BUT WHY  
WOULD THIS BE  
OBTAINED IN  
OPT?

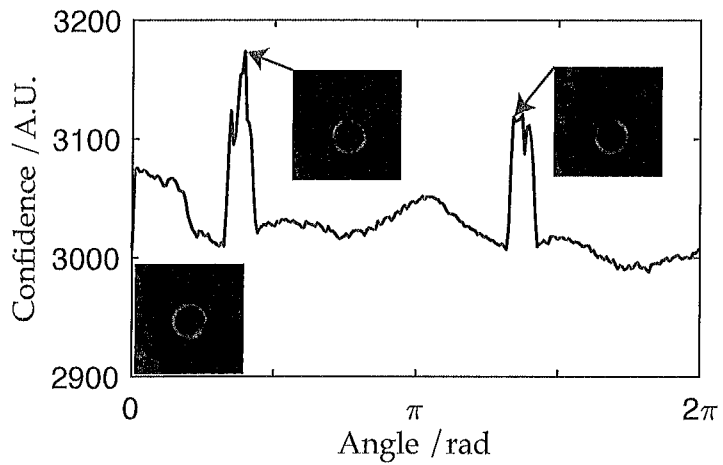


Fig. 4.14 A plot of the confidence value of a single fiducial bead being tracked *in vivo*. Sharp changes in the confidence value occur when the fiducial bead is occluded. The image at the origin shows the fiducial being tracked well in the first frame. (Images courtesy of Pedro Vallejo)

- <sup>1</sup> mathematical framework at present for four or more views. If such tools did exist,
- <sup>2</sup> it may be possible to make the algorithm described above as non-iterative and
- <sup>3</sup> essentially a single shot reconstruction from pixels to voxels.

